

Search for structure in the fusion of $^{28}\text{Si} + ^{28,30}\text{Si}$ and $^{30}\text{Si} + ^{30}\text{Si}$

E. F. Aguilera,* J. J. Kolata, P. A. DeYoung,[†] and J. J. Vega
Physics Department, University of Notre Dame, Notre Dame, Indiana 46556
 (Received 27 January 1986)

Excitation functions for the yields of all the residual nuclei from the $^{28}\text{Si} + ^{28,30}\text{Si}$ and $^{30}\text{Si} + ^{30}\text{Si}$ reactions have been measured via the gamma-ray technique for center of mass energies in the region within one and two times the Coulomb barrier, using steps of 500 keV in the laboratory system. Thirteen nuclides were identified for the first reaction and ten for the other two. While no structure is shown by the data for the $^{28}\text{Si} + ^{28}\text{Si}$ reaction, we have found evidence for intermediate width structure in the 2α and αpn channels in $^{28}\text{Si} + ^{30}\text{Si}$, and for broad structure in the total fusion cross section for $^{30}\text{Si} + ^{30}\text{Si}$. Calculations using a barrier penetration model with one free parameter reproduce the average behavior of the fusion cross sections quite well.

I. INTRODUCTION

The fusion of heavy ions, a phenomenon in which the nucleons of the reacting nuclei drastically rearrange to form a compound nucleus, has captured the interest of many nuclear physicists over a number of years. There are several features of fusion which are not yet well described by the models available. These include the observations of subbarrier fusion,¹⁻⁴ the systematic behavior^{5,6} of the excitation functions for some light systems such as $^{10}\text{B} + ^{16}\text{O}$ and $^{12}\text{C} + ^{14}\text{N}$, and the oscillations observed in the excitation functions for several fusion reactions.⁷⁻⁹

Considerable experimental¹⁰⁻¹⁷ and theoretical¹⁸⁻²¹ effort has been dedicated to studying this last phenomenon, but no coherent explanation of the observations for the different systems has been given, and more work is clearly needed in order to fully understand the underlying physics. In particular, very little experimental work has been done along these lines for systems involving nuclei with $A \geq 50$. A search for possible structure in the fusion of three systems in this not-well-studied mass region was the motivation for this work.

We present here data for the fusion of $^{28}\text{Si} + ^{28,30}\text{Si}$ and $^{30}\text{Si} + ^{30}\text{Si}$, measured with relatively small energy steps (500 keV in the laboratory system), at center of mass energies in the region between one and two times the Coulomb barrier. We used the gamma-ray technique, which allows high accuracy in the measurement of relative cross sections and is therefore particularly appropriate for our purposes. In addition, the technique allows one to clearly identify individual evaporation channels so that a structure which appears preferentially in only one or a few of these channels is more easily detected with this method.

Special interest is attached to the $^{28}\text{Si} + ^{28}\text{Si}$ system on the basis of existing evidence. The observations on many systems seem to indicate a general trend to favor fusion oscillations in reactions where target and projectile are identical alpha-particle nuclei. In addition, for energies above twice the Coulomb barrier the elastic and inelastic scattering of $^{28}\text{Si} + ^{28}\text{Si}$ have revealed striking resonance behavior.²²⁻²⁶ The suggestion of surface-transparent op-

tical potentials as a possible explanation for the observed gross structure²² increases the expectation that oscillations may also appear in the fusion cross sections. Finally, a research for structure in the fusion of this system has been carried out²⁷ but no conclusive results were achieved. We used smaller energy steps and covered a wider energy range than those of the related experiment of Ref. 27.

Additional interest in studying the fusion of $\text{Si} + \text{Si}$ systems comes from the fact that the ground-state shapes are rather different for ^{28}Si and ^{30}Si , being strongly oblate for the first and moderately prolate deformed for the last one. There would be some interest in investigating possible effects of this deformation. Other studies of fusion of $^{28}\text{Si} + ^{30}\text{Si}$ and $^{30}\text{Si} + ^{30}\text{Si}$ have been recently reported,²⁸⁻³⁰ but in none of them has the excitation function been measured with sufficient detail as to produce very conclusive statements about the presence or absence of oscillations.

In the next section we describe the experimental method used in this work. The corresponding results and related discussion for each system are presented in Sec. III, while Sec. IV is dedicated to a comparison with model calculations. Finally, a summary and the conclusions of this work are presented in Sec. V.

II. EXPERIMENTAL TECHNIQUE AND DATA ANALYSIS

The targets, made by vacuum evaporation of enriched ^{28}Si (99.9%, 35 $\mu\text{g}/\text{cm}$) and ^{30}Si (95.2%, 24 $\mu\text{g}/\text{cm}$), were deposited onto a thick Au backing and then covered with a thin Au layer to retard oxidation. Beams of ^{28}Si and ^{30}Si with typical intensities on target of 2 to 3 particle-nanoamps were obtained with the three-stage Van de Graaff facility at the University of Notre Dame. A Ge(Li) detector at 125° to the beam was used in the three experiments to determine the total yields of gamma rays, and another one at 90° was used in the case of $^{28,30}\text{Si} + ^{30}\text{Si}$ for comparison purposes. In order to have a better understanding of our spectra, an investigation of Doppler shift effects was done for $^{28}\text{Si} + ^{28}\text{Si}$ by placing the detector at the symmetric angle 55° and recording

TABLE I. Experiments performed to determine the absolute normalization for $^{28}\text{Si} + ^{28}\text{Si}$, based on the cross section values (Ref. 31) measured by Kolata *et al.* for $^{16}\text{O} + ^{12}\text{C}$.

Projectile	$E_{c.m.}$ (MeV)	Target	γ -ray lines analyzed (keV) and expected result of the analysis
^{16}O	19.3,22.7,24.9	^{12}C	1634(^{20}Ne) target thickness
^{28}Si	21,24,27	^{12}C	3162(^{35}Cl) σ_{abs} for $^{28}\text{Si} + ^{12}\text{C}$
^{12}C	21,24,27	^{28}Si	3162(^{35}Cl) target thickness
^{28}Si	35	^{28}Si	1021(^{49}V) and 1251($^{53}\text{Mn} + ^{51}\text{Mn}$) σ_{abs} for $^{28}\text{Si} + ^{28}\text{Si}$

spectra for five different bombarding energies. The absolute peak efficiencies of the detectors were obtained by using calibration gamma-ray sources (Amersham gamma-ray reference source set No. QCR.1) of $^{57,60}\text{Co}$, ^{88}Y , ^{137}Cs , and ^{133}Ba , placed at the position of the target. A noncalibrated source of ^{56}Co was also used to improve the relative calibration. The dynamic range of the detectors was 100–2700 keV for the $^{28}\text{Si} + ^{28}\text{Si}$ experiment and approximately 100–4500 keV for the other two reactions.

Observed deviations in the collected charge, amounting to less than 2%, were corrected for by a relative normalization procedure assuming a smooth energy behavior of the Coulex of gamma-ray lines from the Au backing. The absolute normalization factors were obtained by using appropriate combinations of targets and projectiles to scale the relevant cross sections to those measured³¹ for the 1634 keV line (^{20}Ne) from $^{16}\text{O} + ^{12}\text{C}$. The method is illustrated in Table I, where the reactions involved in the absolute normalization of $^{28}\text{Si} + ^{28}\text{Si}$ are summarized. Charge collection errors will approximately cancel in this method due to their expected bias toward positive values and to the fact that only ratios of charges appear in the scaling formula. Results consistent with these expectations were obtained when calculated Coulex yields were used instead of the integrated charge to compute³² the number of projectiles relevant to the absolute normalization of the $^{28}\text{Si} + ^{28}\text{Si}$ reaction. This gave a normalization factor differing from the previous one by less than 2%.

Identification of the gamma-ray lines was accomplished by matching observed and reported gamma-ray energies, checking consistency with published branching ratios whenever relevant.³³ Beam-off spectra were also recorded, providing a cross check for the identification through the known beta-decay schemes. In addition, in each case a comparison of excitation functions was done for several lines assigned to the same residue, as a final test of consistency in the identification. Finally, a gamma-gamma coincidence experiment at 75 MeV beam energy was performed for $^{30}\text{Si} + ^{30}\text{Si}$ to verify the reliability of the procedure. A total of 22.5×10^6 events were recorded on tape for this experiment, with a time resolution of 100 ns. The corresponding results will be discussed below in Sec. III. The production cross sections for the reaction residues were determined from gamma-ray yields corresponding to

the respective ground state transitions (or approximations to them), as indicated in Table II.

It was impossible to completely eliminate oxygen contamination of our targets and it was thus necessary to measure the reactions $^{28}\text{Si} + ^{16}\text{O}$ and $^{30}\text{Si} + ^{16}\text{O}$, at the same energies as in the original experiments, in order to correct the data. The lines at 756 keV ($^{39}\text{K} + ^{36}\text{Ar}$) in the first reaction, and at 1704 keV (^{44}Sc) in the second one,

TABLE II. Identified residues and gamma-ray lines used to obtain the corresponding excitation functions.

Residue	Lines used (keV)	Notes
^{46}Ti	888 ^d	(a)
^{47}V	1148	(a)
^{48}V	427,626 ^e	(a)
^{48}Cr	751	(a)
^{49}V	1021	(a),(b,g)
^{49}Cr	271,1084 ^e	(a),(b,g,h)
^{50}Cr	782	(a,d),(b,d,g),(c,g)
^{51}Cr	1163,1480	(a),(b,g),(c,e,g)
^{52}Cr	1434	(b,i),(c,g)
^{51}Mn	237 ^f ,1139 ^e	(a)
^{52}Mn	870,2286 ^e	(b,g)
^{53}Mn	1440	(a),(b,g),(c,g)
^{54}Mn	213	(b),(c,g)
^{53}Fe	700 ^f	(a)
^{54}Fe	1409 ^d	(a),(b,f),(c,g)
^{55}Fe	1317	(b,e),(c,e,g)
^{56}Fe	846	(c)
^{57}Fe	870,992,1061	(c)
^{57}Co	1223,1690	(c,e)

^aAnalyzed in $^{28}\text{Si} + ^{28}\text{Si}$.

^bAnalyzed in $^{28}\text{Si} + ^{30}\text{Si}$.

^cAnalyzed in $^{30}\text{Si} + ^{30}\text{Si}$.

^dA contribution from O contamination was subtracted.

^eThis determination involves reported branching ratios.

^fA correction for activity from a long-lived state was made.

^gA contribution from ^{28}Si contaminant was subtracted.

^hThe yield in the 271 keV line was estimated from the sum of the yields in the lines at 812 and 1289 keV, corrected for O contamination.

ⁱThe 1163 keV line was used instead of the one at 1434 keV.

were used to scale the corresponding excitation functions to those in the contaminated Si targets. Estimations for activity contamination were also made whenever pertinent and in some cases corresponding corrections were applied (see Table II). Further details of the experimental procedure have been extensively described in Ref. 32.

III. RESULTS AND DISCUSSION

A. $^{28}\text{Si} + ^{28}\text{Si}$ system

Thirteen residual nuclei were identified in this work as resulting from the $^{28}\text{Si} + ^{28}\text{Si}$ reaction. This corresponds to more than double the number of evaporation channels reported by Medsker *et al.*³⁴ for the same reaction, and to five additional residues as compared to the more complete work by DiCenzo *et al.*,²⁷ who did not identify any of the four-particle [$^{46}\text{Ti}(2\alpha 2p)$ and $^{49}\text{Cr}(\alpha 2pn)$] or five-particle [$^{48}\text{V}(\alpha 2p 2n)$ and $^{51}\text{Cr}(4pn)$] channels.

The excitation functions corresponding to the eight more prominent residues are presented in Fig. 1. Except for ^{54}Fe , the yields of all the remaining channels are still rising at the highest energies we measured, with approximate maxima of 70, 65, 47, and 18 mb for ^{47}V , ^{51}Cr , ^{48}V , and ^{48}Cr , respectively. The yield of ^{54}Fe peaks near 70 MeV in the laboratory system, with a maximum of approximately 30 mb.

The overall shapes of the excitation functions obtained by DiCenzo *et al.*²⁷ are generally in good agreement with ours in the region of common energies. Large discrepancies exist in the corresponding absolute values, however, which can probably be traced back to the fact that no correction was made for oxygen contamination in Ref. 27 (although gamma-ray lines from that source are apparent in the spectrum they present), and that their normalization procedure was sensitive to the missing flux corresponding to nonidentified channels. According to our results, these channels make a contribution of about 120 mb to the total cross section at the energy they picked to normalize (80 MeV).

A more sensitive test is to compare our total cross sections to the results they obtained by particle detection techniques, which presumably give more reliable absolute values. This is done in Fig. 2, which also shows the data of Gary and Volant²⁸ obtained in another particle detection experiment. Except for the highest energy point, the agreement with the data from Ref. 27 is excellent. A tendency of the gamma-ray data to underestimate the total cross sections at high energies has been observed in other work (see, for example, Figs. 22 and 25 in Ref. 35). The possible explanation in terms of unidentified channels does not seem probable in our case since great care was taken in the identification. More plausible is the fact that many channels might be opening in this high energy region which populate mainly ground states of new residues and are thus undetectable by our technique.

The comparison with the data of Gary and Volant, on the other hand, shows a discrepancy of about 15% over most of the range of common energies which includes the lowest energy point of Ref. 27. These authors have also reported, for a few energies, a separation of residues in groups of masses corresponding to $(0\alpha + x)$ nucleons,

and $(2\alpha + z)$ nucleons). The comparison with these more detailed data, presented in Fig. 3, shows fairly good agreement in the overall distributions. This indicates that the above-mentioned discrepancy in the absolute cross sections is most probably due to a problem of absolute normalization.

Finally, we note that none of the excitation functions in

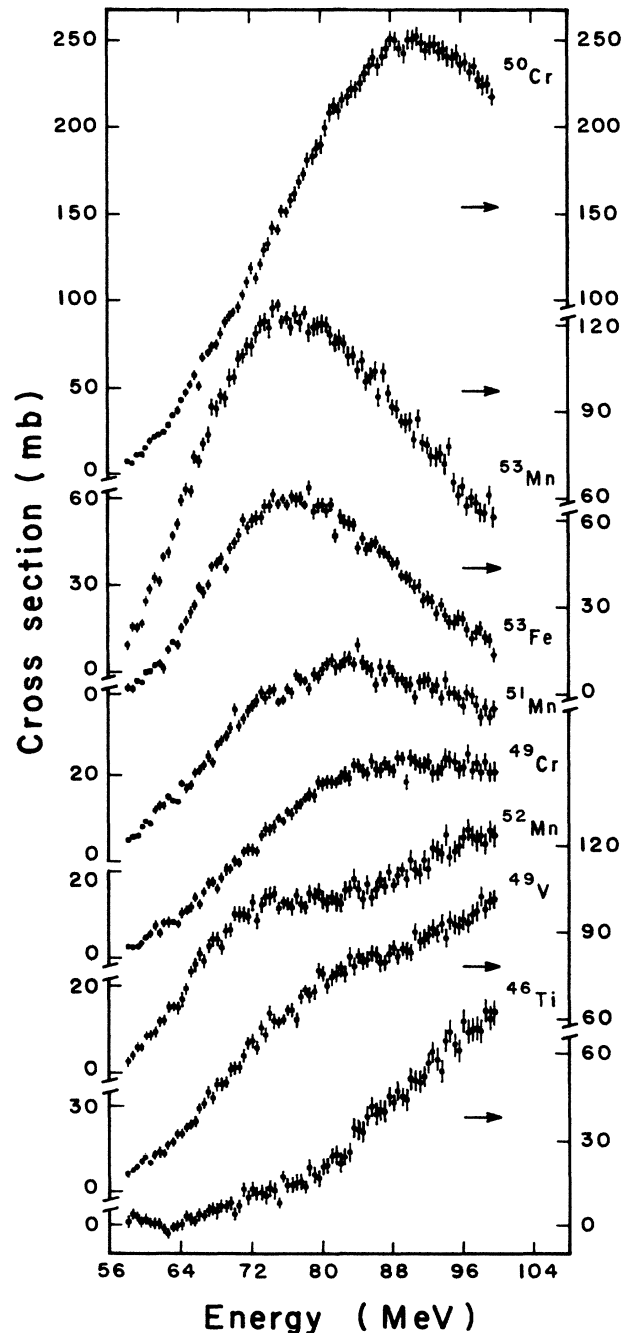


FIG. 1. Excitation functions for the eight more prominent evaporation channels from the $^{28}\text{Si} + ^{28}\text{Si}$ reaction.

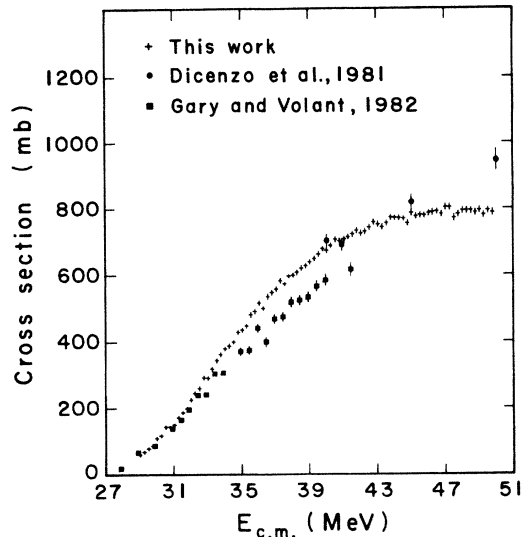


FIG. 2. Total cross sections obtained in this work for the fusion of $^{28}\text{Si} + ^{28}\text{Si}$ (+). Also shown are the results of Refs. 27 (●) and 28 (■).

our experiment shows a behavior that could be considered as a nonstatistical oscillation. In particular, the possible structures in the ^{50}Cr excitation function at 92 and 97 MeV reported by DiCenzo *et al.* are not seen in our data, in spite of the smaller energy steps. These authors found indications of correlated structures at these two energies for the transitions at 610, 783, 1098, and 1283 keV in ^{50}Cr . The possible presence of ^{50}Mn in the reaction^{32,34} would offer an explanation for this since the last three lines are present in the decay of ^{50}Mn . The energies at which a "structure" originating in the decay is observed

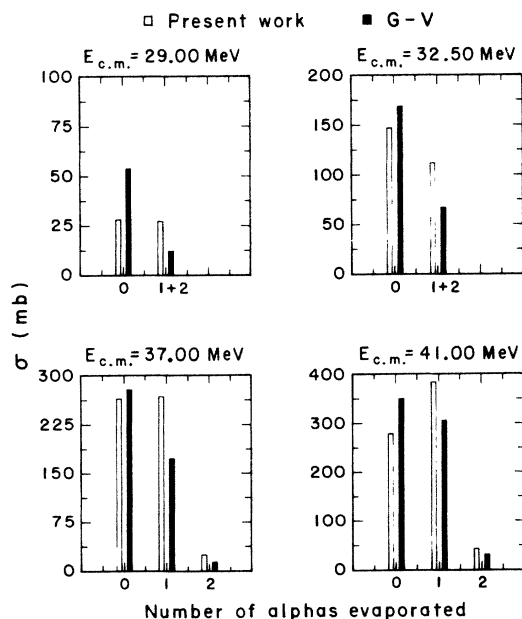


FIG. 3. Residue distributions in $^{28}\text{Si} + ^{28}\text{Si}$ according to the number of α particles evaporated from the compound nucleus. Our results are compared with those of Ref. 28.

would then depend on the detailed history of the experiment, which in turn would explain why we did not see such structure. Alternatively, the observed results could be the effect of purely random fluctuations, as the same authors have pointed out.

B. $^{28}\text{Si} + ^{30}\text{Si}$ system

The excitation functions for eight of the more prominent evaporation channels from the $^{28}\text{Si} + ^{30}\text{Si}$ reaction are presented in Fig. 4. As to the other two identified channels, the yield of the $2\alpha n$ channel (^{49}Cr) is essentially

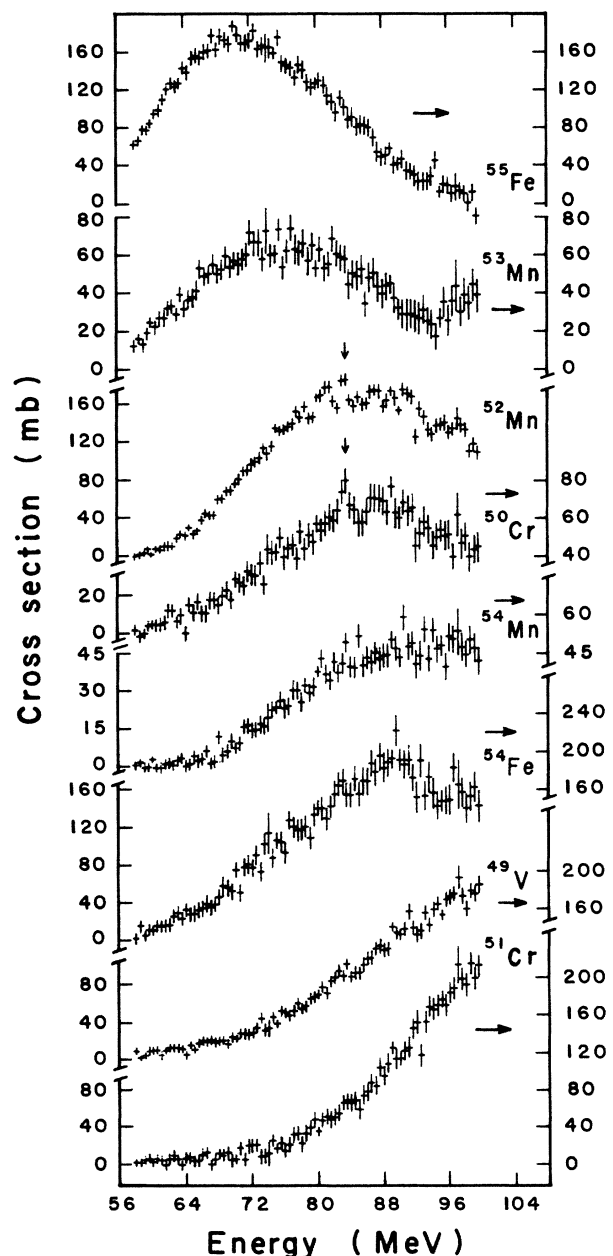


FIG. 4. Excitation functions for the eight more prominent evaporation channels from the $^{28}\text{Si} + ^{30}\text{Si}$ reaction.

zero up to 80 MeV, where it begins to rise rapidly and attains a maximum of ~ 120 mb at the higher energies. The yield for ^{52}Cr , on the other hand, shows a maximum of ~ 60 mb at 90 MeV.

An apparent structure having a peak-to-valley ratio of more than 15% is suggested in this figure for the 2α (^{52}Mn) and the αpn (^{50}Cr) channels, both of which show a sharp peak at 83.5 MeV. To further investigate this possibility, a correlation analysis was made for the lines at 783, 1098, and 1283 keV in ^{50}Cr and those at 870 and 930 keV in ^{52}Mn , the more statistically significant lines from these nuclides.

The cross correlation function, defined by²⁷

$$C(E) = \frac{2}{N(N-1)} \sum_{i>j=1}^N \frac{D_i(E)D_j(E)}{\gamma_i(E)\gamma_j(E)},$$

where

$$D_i(E) = \frac{\sigma_i(E) - \langle \sigma_i(E) \rangle}{\langle \sigma_i(E) \rangle}$$

and

$$\gamma_i^2(E) = \langle D_i^2(E) \rangle,$$

was calculated for the five excitation functions using an averaging interval of 11 points, centered at the energy of interest. The corresponding results, presented in Fig. 5, show an actual correlation at $E=83.5$ MeV, where the respective value differs from zero by more than four standard deviations. Other possible (weaker) correlated structure becomes evident in Fig. 5 at 89, 90.5, and 92 MeV, but the cross correlation function differs from zero by only a little more than two standard deviations at these energies. It would be highly desirable to have more points

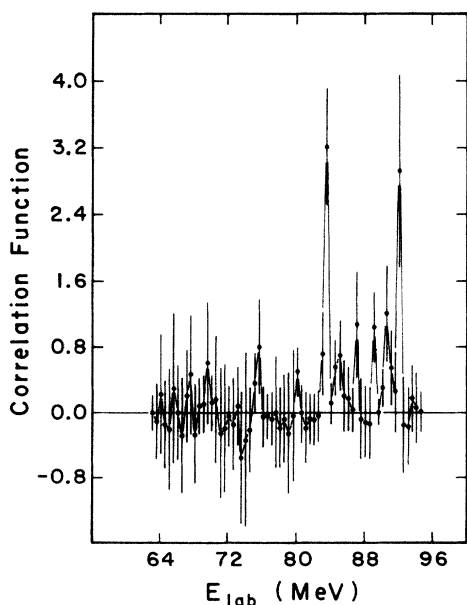


FIG. 5. Cross correlation function for the yields of the lines at 870 and 930 keV in ^{52}Mn and the lines at 783, 1098, and 1283 keV in ^{50}Cr , as measured in the $^{28}\text{Si} + ^{30}\text{Si}$ experiment.

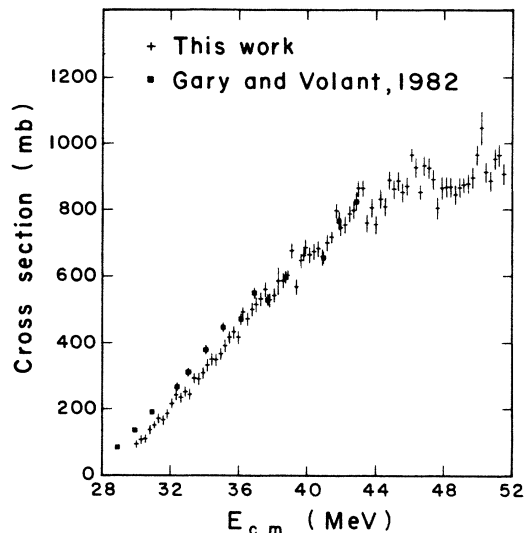


FIG. 6. Total cross sections obtained in this work for the fusion of $^{28}\text{Si} + ^{30}\text{Si}$ (+). Also shown are the results of Ref. 28 (■).

in this energy region, with better statistics, in order to corroborate the presence of this seemingly rich structure, which on the other hand appears to be preserved in the excitation function for the total cross section presented in Fig. 6.

No data for individual excitation functions have been previously published for this system, but total cross sections have been recently reported in two works.^{28,29} In Fig. 6 we compare the total cross sections obtained in this work with those measured by Gary and Volant²⁸ using particle detection techniques. The agreement is excellent over most of the energy range, but the two sets of data start to diverge from each other at the lowest energies. Since we have only a very small error in our relative normalization (less than 2%), two possibilities arise: either there is a relative normalization problem in Ref. 28 (the authors do mention the possibility of having big errors at low energies), or more residues are being populated directly in their ground states at these energies and are consequently being missed in our work.

A direct comparison with the data of Ref. 29 (obtained with gamma-ray techniques) would be difficult to make because of the way they present the data. Although the authors claim to have good agreement with the data from Gary and Volant, their reported errors bars of more than 20% would make it impossible to resolve the discrepancy with our data in the low energy region.

C. $^{30}\text{Si} + ^{30}\text{Si}$ system

The identification procedure followed in this work was proved to be reliable with the help of the gamma-gamma coincidence experiment performed on the $^{30}\text{Si} + ^{30}\text{Si}$ system. The information contained in all the coincidence spectra analyzed (gates were set³² on more than 40 lines, covering all the observed residues) was found to be con-

sistent with the corresponding level schemes published in the literature.³³ Only the two lines at 329 and 2289 keV, which are assigned to ^{57}Co in this experiment, had not been to our knowledge previously reported. Our data strongly suggest that both these transitions feed the state at 2524 keV, which would mean that two nonreported states exist in ^{57}Co , at energies of 2847 and 4813 keV, respectively. A state at 4805 keV, which could coincide with the one suggested at 4813 keV, has been reported in Ref. 36. A more detailed experiment is needed to corroborate this hypothesis.

Excitation functions for ten residues from the $^{30}\text{Si} + ^{30}\text{Si}$ reaction were obtained, from which the seven more prominent ones are presented in Fig. 7. Of the

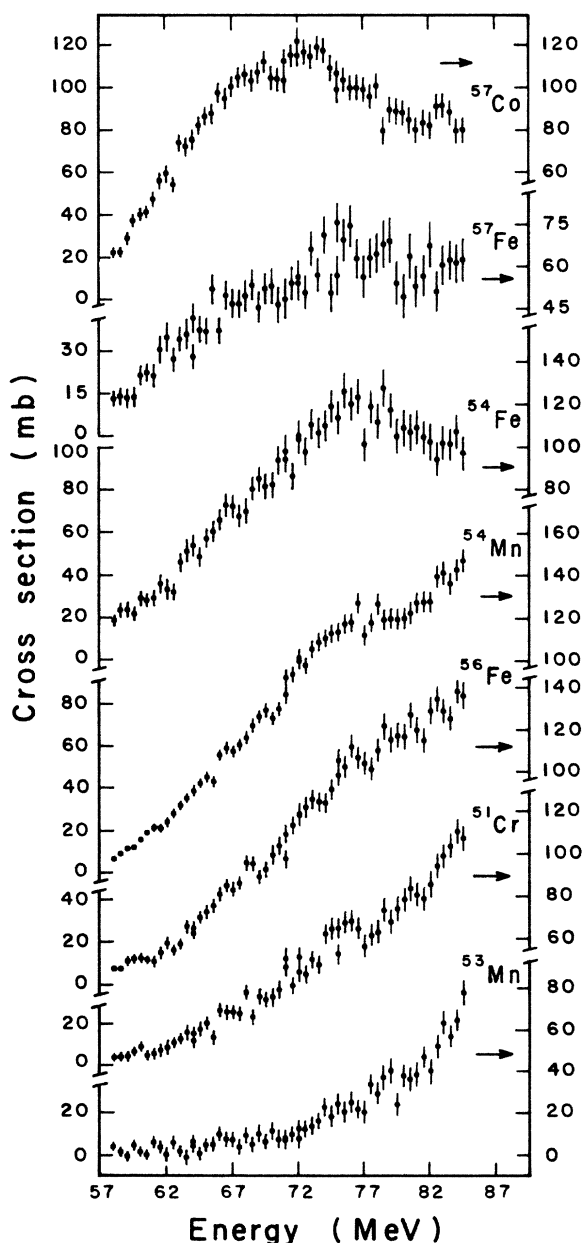


FIG. 7. Excitation functions for the seven more prominent evaporation channels from the $^{30}\text{Si} + ^{30}\text{Si}$ reaction.

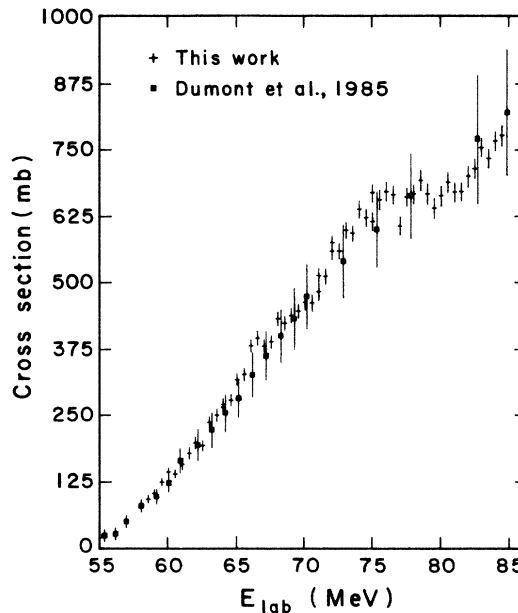


FIG. 8. Total fusion cross sections obtained in this work for the $^{30}\text{Si} + ^{30}\text{Si}$ reaction (+). Also shown (■) are the results of Ref. 30.

remaining three evaporation channels, ^{50}Cr and ^{52}Cr show similar behavior in that their yields increase with increasing energy in all the measured range, with maxima of 17 and 34 mb, respectively. The yield for ^{55}Fe , on the other hand, displays a maximum of ~ 28 mb at 78 MeV bombarding energy.

No obvious structure is shown by the data for the individual evaporation channels in the energy range studied. However, when the yields are summed to obtain the total cross section (Fig. 8), a broad structure becomes apparent in the region above 36 MeV c.m. energy, giving a fluctuation of about 10% with respect to the average behavior. This structure is reminiscent of that observed by Kolata *et al.*³⁷ for $^{16}\text{O} + ^{16}\text{O}$ which could be qualitatively explained in terms of shape resonances in the optical potential.

Total fusion cross sections for $^{30}\text{Si} + ^{30}\text{Si}$ have been recently reported^{29,30} and the corresponding data are also presented in Fig. 8 for comparison. Even though no structure is apparent in these data, the agreement with our results is very good and certainly no inconsistency exists between the two data sets if the reported errors are taken into account.

IV. COMPARISON WITH MODEL CALCULATIONS

The barrier penetration model provides a suitable framework to analyze total fusion cross sections in the range of energies we studied. In this model, based on the assumption of friction-free passage over or through the one-dimensional barrier, the fusion cross section is given by

$$\sigma_{\text{fus}} = \pi \lambda^2 \sum_{l=0}^{\infty} (2l+1) T_l.$$

Following Vaz and co-workers,^{1,38,39} the transmission coefficients are calculated by approximating the barrier with an inverted parabola and using the formula of Hill and Wheeler⁴⁰

$$T_l(E) = \left[1 + \exp \left\{ \frac{2l}{\hbar\omega_l} [V_l(R_l) - E] \right\} \right]^{-1},$$

where R_l and $\hbar\omega_l$ are the radius and the curvature of the barrier, respectively.

The nucleus-nucleus potential is written as the sum of the Coulomb potential of a point charge and spherical charge distribution, plus the nuclear proximity potential of Blocki *et al.*⁴¹ The equivalent sharp surface radii used in this last potential are modified by an additive parameter ΔR , which is varied until the best visual match is achieved with the measured fusion cross sections in the range $100 < \sigma < 500$ mb. With this procedure, Vaz *et al.*¹ were able to obtain barrier parameters which are almost independent of the assumed Coulomb and nuclear potentials.

The total effective potential used for $^{28}\text{Si} + ^{28}\text{Si}$ is shown in the upper left corner of Fig. 9 for the angular momenta $l=0$ and $l=32$. A value of 0.15 fm for ΔR has been used here based on the comparison with experimental results to be discussed below. The corresponding barrier parameters are plotted in the lower part of the figure for the whole range of angular momenta relevant in our experiment. This range is determined in the upper right part of the figure, which shows the transmission coefficients obtained in this model for the maximum experimental energy we used. The fact that a pocket is still shown by the effective potential for $l=32$ verifies that the conditions necessary for the applicability of the barrier penetration model are still satisfied by our experimental systems.

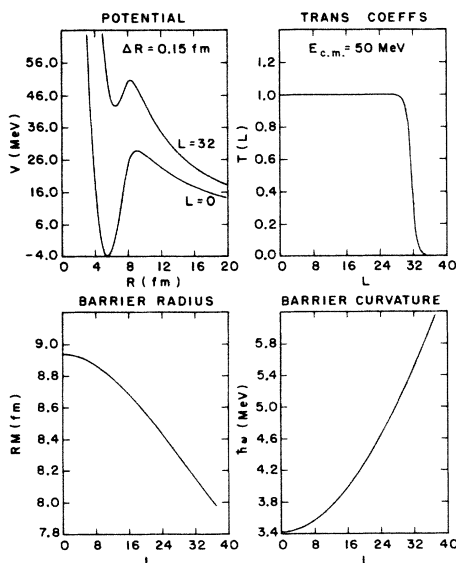


FIG. 9. Ingredients in the barrier penetration model for the $^{28}\text{Si} + ^{28}\text{Si}$ system. A further description is given in the text.

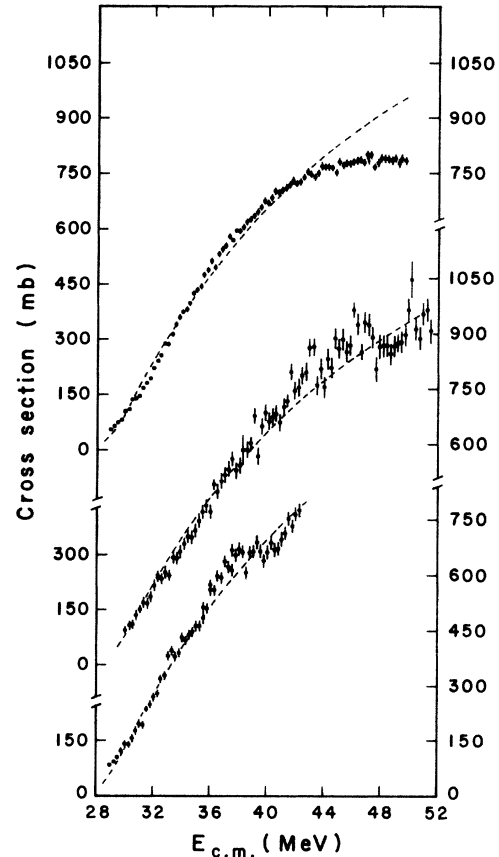


FIG. 10. Comparison of experimental fusion cross sections with predictions of the barrier penetration model (dashed line). (a) $^{28}\text{Si} + ^{28}\text{Si}$, (b) $^{28}\text{Si} + ^{30}\text{Si}$, (c) $^{30}\text{Si} + ^{30}\text{Si}$.

The general trend of our data is well reproduced by the model predictions, as shown in Fig. 10. The small deviations apparent for $^{28}\text{Si} + ^{28}\text{Si}$ below 44 MeV are probably due to complexities in the low energy fusion mechanism not accounted for in this model.¹ Above this energy, there seems to be a yield undetectable by our technique, as was commented on earlier. In the case of the $^{28}\text{Si} + ^{30}\text{Si}$ and $^{30}\text{Si} + ^{30}\text{Si}$ systems, the deviations from the smooth curve provided by the model are associated with the structure previously discussed.

The corresponding barrier parameters are shown in Table III along with a comparison with the systematics of Vaz *et al.*,¹ who analyzed 87 reactions and obtained empirical expressions for the reduced parameters

$$r_{ef} \equiv Z_T Z_P e^2 / V_0 (A_T^{1/3} + A_P^{1/3})$$

and

$$r_{of} \equiv R_0 / (A_T^{1/3} + A_P^{1/3}).$$

We see from the sixth and seventh columns in Table III that the barrier parameters obtained in this work follow the systematic trends quite well.

TABLE III. Empirical parameters (defined in the text) obtained from our data using the barrier penetration model. (The corresponding calculated curves are shown in Fig. 10.)

System	ΔR (fm)	R_0 (fm)	V_0 (MeV)	$\hbar\omega_0$ (MeV)	r_{ef}/\bar{r}_{ef}	r_{of}/\bar{r}_{of}
$^{28}\text{Si} + ^{28}\text{Si}$	0.15	8.94	28.89	3.42	0.99	0.99
$^{28}\text{Si} + ^{30}\text{Si}$	0.08	8.86	29.13	3.39	0.98	0.97
$^{30}\text{Si} + ^{30}\text{Si}$	0.11	9.06	28.54	3.26	0.98	0.97

A comparison with barrier parameters reported in other work is shown in Table IV. In Refs. 27 and 28, a fitting of the classical formula to the data was made in order to extract the barrier parameters. Reference 5 gives theoretical values calculated from a modified proximity potential and the Coulomb potential of Bondorf *et al.*,⁴² without any fit to fusion data. References 1 and 29 both follow essentially the same procedure that we did and therefore the comparison with their values does actually test the overall equivalence of the experimental data. The good agreement between our parameters and those associated with these references in the table is consistent with the more direct comparisons discussed in Sec. III.

V. SUMMARY AND CONCLUSIONS

The fusion of the three systems $^{28}\text{Si} + ^{28,30}\text{Si}$ and $^{30}\text{Si} + ^{30}\text{Si}$ has been studied in this work via the gamma-ray technique. Careful classification of all the observed gamma-ray lines led to the positive identification of all the relevant evaporation channels for each reaction. With the help of gamma-gamma coincidence measurements, two new transitions were discovered in ^{57}Co .

Yields for 13 residues from the $^{28}\text{Si} + ^{28}\text{Si}$ reaction were obtained in this work, five of which had not been measured before. Excitation functions for ten evaporation channels observed from each of the other two reactions are reported for the first time.

The possibility of oscillations suggested for the $^{28}\text{Si} + ^{28}\text{Si}$ system by the results of previous observations²² was ruled out here, as no structure that could be resolved within the 3% error bars was observed in our work. A

possible delayed decay was suggested to account for the different observations. This lack of structure is significant in view of the work of Saini and Betts,²⁶ who observe a series of broad structures ($\Gamma_{c.m.} = 1-2$ MeV) in the elastic and inelastic scattering channels of $^{28}\text{Si} + ^{28}\text{Si}$ at energies ($E_{c.m.} = 52-62$ MeV) which are just above those investigated in the present experiment. Each of these broad structures was fragmented into a number of much narrower resonances ($\Gamma_{c.m.} = 100-300$ keV). They interpret these observations as being qualitatively consistent with the picture of broad structures, arising from a series of shape resonances in the entrance channel, which are fragmented by mixing with states of a more complex nature. In the $^{16}\text{O} + ^{16}\text{O}$ system, where a similar situation occurs, the anomalies in the elastic and inelastic channels are accompanied by broad resonances in the total fusion cross section.³⁷ While our experimental energy resolution in the present work is insufficient to resolve the narrow resonances observed by Saini and Betts, we would expect to have been able to see the underlying broad shape resonances clearly if they appeared in the total fusion yield, and in fact we did observe broad oscillations in the $^{28}\text{Si} + ^{30}\text{Si}$ and $^{30}\text{Si} + ^{30}\text{Si}$ fusion cross sections. The absence of structure for $^{28}\text{Si} + ^{28}\text{Si}$ is therefore quite surprising.

In the case of the $^{28}\text{Si} + ^{30}\text{Si}$ reaction, a correlated structure at 83.5 MeV, having a peak-to-valley ratio of more than 15% and a width of about 1 MeV, was observed for the 2α and αpn channels. Evidence for more structure (weaker) of about the same width was also found for the same channels in the region above this energy.

No obvious structure appeared in the yields for indi-

TABLE IV. Comparison with barrier parameters obtained in other works.

$^{28}\text{Si} + ^{28}\text{Si}$			$^{28}\text{Si} + ^{30}\text{Si}$			$^{30}\text{Si} + ^{30}\text{Si}$		
R_0 (fm)	V_0 (MeV)	Ref.	R_0 (fm)	V_0 (MeV)	Ref.	R_0 (fm)	V_0 (MeV)	Ref.
8.94	28.89	a	8.86	29.13	a	9.06	28.54	a
9.08	29.6	b	8.82	29.27	f	9.02	28.68	f
8.25	28.95	c	8.47	28.28	c			
8.63	29.83	d	8.75	29.38	d			
9.06	28.67	e,b,g						

^aThis work.

^bReference 27.

^cReference 28.

^dReference 5.

^eReference 1.

^fReference 29.

^gDetermined in Ref. 1 with data from Ref. 28.

vidual residues from the $^{30}\text{Si} + ^{30}\text{Si}$ reaction, but a broad oscillation was observed in the total fusion cross section extending from about 36 to 42.5 MeV c.m. energy, giving a fluctuation of about 10% with respect to the average behavior. This reminds one of the similar structure observed in lighter identical-particle systems, which could share a common origin.

Comparison with total cross sections measured in other work generally showed good agreement except for the case of $^{28}\text{Si} + ^{28}\text{Si}$, where a discrepancy already existed between the results of two published works. The agreement of our data with one of these works thus contributes to the solution of the existing ambiguity.

The general trends of our data are well described by the predictions of a simple barrier penetration model in which the barrier in the Coulomb plus proximity potential is approximated with an inverted parabola. By varying only one parameter in this potential, empirical barrier parameters are extracted which follow very well the systematic

trends obtained from a large number of other reactions.

In summary, our results seem to indicate that the observed tendency for preferential structure in the fusion of identical nuclei is not valid for Si + Si systems. Further experimental work suggested by this study would include a more detailed investigation of $^{28}\text{Si} + ^{30}\text{Si}$ in the region between 40 and 50 MeV c.m. energy, where a rich structure is apparent in our data. It would be also very interesting to extend our measurements on $^{30}\text{Si} + ^{30}\text{Si}$ to higher energies, where additional oscillatory behavior might be expected from our results, and to carry out similar measurements on the $^{28}\text{Si} + ^{28}\text{Si}$ system over the energy range investigated by Saini and Betts, to see if the expected broad oscillations suddenly appear at $E_{\text{c.m.}} = 52$ MeV and above.

This work was supported by the National Science Foundation under Grant No. PHY84-21302.

*Present address: Instituto Nacional de Investigaciones Nucleares, Mexico City, Mexico, D.F.

†Present address: Physics Department, Hope College, Holland, MI 49423.

¹L. C. Vaz, J. M. Alexander, and G. R. Satchler, *Phys. Rep.* **69**, 373 (1981).

²L. C. Vaz, J. M. Alexander, M. Prakash, and S. Y. Lee, in *Nuclear Physics with Heavy Ions*, edited by P. Braun-Munzinger (Harwood, New York, 1984), Vol. 6, p. 31.

³M. Beckerman, in Ref. 2, p. 289.

⁴S. E. Koonin, Proceedings of the National Summer School for Nuclear Physics, Georgetown University, 1985 (unpublished).

⁵J. R. Birkelund and J. R. Huizenga, *Annu. Rev. Nucl. Part. Sci.* **33**, 265 (1983).

⁶J. Gomez del Campo, J. A. Biggerstaff, R. A. Dayras, D. Shapira, A. H. Snell, P. H. Stelson, and R. G. Stokstad, *Phys. Rev. C* **29**, 1722 (1984).

⁷W. Henning, in *Dynamics of Heavy Ion Collisions*, edited by N. Cindro *et al.* (North-Holland, Amsterdam, 1981), p. 75.

⁸*Resonances in Heavy Ion Reactions, Lecture Notes in Physics 156* (Springer, Berlin, 1982).

⁹T. M. Cormier, *Annu. Rev. Nucl. Part. Sci.* **32**, 271 (1982).

¹⁰D. G. Kovar, D. F. Geesaman, T. H. Braid, Y. Eisen, W. Henning, T. R. Ophel, M. Paul, K. E. Rehm, S. J. Sanders, P. Sperr, J. P. Schiffer, S. L. Tabor, S. Vigdor, B. Zeidman, and F. W. Prosser, Jr., *Phys. Rev. C* **20**, 1305 (1979).

¹¹J. J. Kolata, R. M. Freeman, F. Haas, B. Heusch, and A. Gallmann, *Phys. Rev. C* **19**, 408 (1979).

¹²J. J. Kolata, R. M. Freeman, F. Haas, B. Heusch, and A. Gallmann, *Phys. Rev. C* **19**, 2237 (1979).

¹³P. A. DeYoung, J. J. Kolata, R. C. Luhn, R. E. Malmin, and S. E. Tripathi, *Phys. Rev. C* **25**, 1420 (1982).

¹⁴K. Daneshvar, D. G. Kovar, S. J. Krieger, and K. T. R. Davies, *Phys. Rev. C* **25**, 1342 (1982).

¹⁵R. A. Racca, P. A. DeYoung, J. J. Kolata, and R. J. Thornburg, *Phys. Lett.* **129B**, 294 (1983).

¹⁶P. Pocanic and N. Cindro, in *Dynamics of Heavy Ion Collisions*, edited by N. Cindro *et al.* (North-Holland, Amsterdam, 1981), p. 101.

¹⁷J. J. Kolata, R. A. Racca, P. A. DeYoung, E. Aguilera Reyes,

and M. A. Xapsos, *Phys. Rev. C* **32**, 1080 (1985).

¹⁸R. Vandenbosch, *Phys. Lett.* **87B**, 183 (1979).

¹⁹Y. Kondo, D. A. Bromley, and Y. Abe, *Phys. Rev. C* **22**, 1068 (1980).

²⁰R. Vandenbosch and A. J. Lazzarini, *Phys. Rev. C* **23**, 1074 (1981).

²¹Q. Haider and F. B. Malik, *Phys. Rev. C* **28**, 2328 (1983).

²²R. R. Betts, S. B. DiCenzo, and J. F. Petersen, *Phys. Rev. Lett.* **43**, 253 (1979).

²³R. R. Betts, B. B. Back, and B. G. Glagola, *Phys. Rev. Lett.* **47**, 23 (1981).

²⁴R. R. Betts and S. Saini, *Phys. Scr.* **15**, 204 (1983).

²⁵R. R. Betts, in Ref. 2, p. 347.

²⁶S. Saini and R. R. Betts, *Phys. Rev. C* **29**, 1769 (1984).

²⁷S. B. DiCenzo, J. F. Petersen, and R. R. Betts, *Phys. Rev. C* **23**, 2561 (1981).

²⁸S. Gary and C. Volant, *Phys. Rev. C* **25**, 1877 (1982).

²⁹D. M. DeCastro Rizzo, E. Bozek, S. Cavallaro, B. Delaunay, J. Delaunay, H. Dumont, M. G. Saint-Laurent, and F. Terrasi, *Nucl. Phys.* **A427**, 151 (1984).

³⁰H. Dumont, B. Delaunay, F. Delaunay, D. M. DeCastro Rizzo, A. Brondi, P. Cuzzocrea, A. D'Onofrio, R. Moro, M. Romano, and F. Terrasi, *Nucl. Phys.* **A435**, 301 (1985).

³¹J. J. Kolata, R. M. Freeman, F. Haas, B. Heusch, and A. Gallman, *Phys. Lett.* **65B**, 333 (1976).

³²E. F. Aguilera, Ph.D. dissertation, University of Notre Dame, 1985.

³³Gamma ray energies and/or branching ratios can be found in: I. Tables ordered by gamma-ray energy and/or nuclide: (1) ($A=6$ to $A=20$) R. J. deMeijer and H. S. Plendl, *At. Data Nucl. Data Tables (ADNDT)* **13**, 1 (1974); (2) ($A=21$ to $A=32$) R. J. de Meijer, A. G. Drentje, and H. S. Plendl, *ADNDT* **15**, 391 (1975); (3) ($A=33$ to $A=44$) R. J. DeMeijer and A. G. Drentje, *ADNDT* **17**, 211 (1976); (4) ($A=32$ to $A=46$) E. K. Warburton, J. J. Kolata, J. W. Olness, A. R. Poletti, and Ph. Gorodetzky, *ADNDT* **14**, 147 (1974). II. Energy-level schemes: (1) (all A) *Table of Isotopes*, 7th ed., edited by C. M. Lederer and V. S. Shirley (Wiley, New York, 1978); (2) ($A=18-20$) F. Ajzenberg-Selove, *Nucl. Phys.* **A392**, 1 (1983); (3) ($A=21-44$) P. M. Endt and C. Van der

- Leun, Nucl. Phys. **A310**, 1 (1978); (4) ($A > 44$) Nuclear Data Sheets.
- ³⁴L. R. Medsker, L. V. Theisen, L. H. Fry, Jr., and J. S. Clements, Phys. Rev. C **20**, 790 (1979).
- ³⁵J. R. Birkelund, L. E. Tubbs, J. R. Huizenga, J. N. De, and D. Sperber, Phys. Rep. **56**, 107 (1979).
- ³⁶J. F. Mateja, J. A. Bieszk, J. T. Meek, J. T. Goss, A. A. Rollefson, P. L. Jolivet, and C. P. Browne, Phys. Rev. C **13**, 2269 (1976).
- ³⁷J. J. Kolata, R. C. Fuller, R. M. Freeman, F. Haas, B. Heusch, and A. Gallmann, Phys. Rev. C **16**, 891 (1977).
- ³⁸L. C. Vaz, J. M. Alexander, and E. H. Auerbach, Phys. Rev. C **18**, 820 (1978).
- ³⁹K. Siwek-Wilczynska and J. Wilczynski, Phys. Lett. **74B**, 313 (1978).
- ⁴⁰D. L. Hill and J. A. Wheeler, Phys. Rev. **89**, 1102 (1953).
- ⁴¹J. Blocki, J. Randrup, W. J. Swiatecki, and C. F. Tsang, Ann. Phys. (N.Y.) **105**, 427 (1977).
- ⁴²J. P. Bondorf, M. I. Sobel, and D. Sperber, Phys. Rep. **15**, 83 (1974).